1-2021

Biocultural Evidence of Precise Manual Activities in an Early Holocene Individual of the High-Altitude Peruvian Andes

Fotios Alexandros Karakostis
University of Tübingen, Germany

Hugo Reyes-Centeno
University of Kentucky, hugo.reyes-centeno@uky.edu

Michael Franken
State Office for Cultural Heritage Baden-Württemberg, Germany

Gerhard Hotz
Natural History Museum of Basel, Switzerland

Kurt Rademaker
Michigan State University

See next page for additional authors

Biocultural Evidence of Precise Manual Activities in an Early Holocene Individual of the High-Altitude Peruvian Andes

Digital Object Identifier (DOI)
https://doi.org/10.1002/ajpa.24160

Notes/Citation Information

Published in *American Journal of Physical Anthropology*, v. 174, issue 1.

Authors

Fotios Alexandros Karakostis, Hugo Reyes-Centeno, Michael Franken, Gerhard Hotz, Kurt Rademaker, and Katerina Harvati

Received: 23 April 2020 | Revised: 12 September 2020 | Accepted: 2 October 2020

DOI: 10.1002/ajpa.24160

RESEARCH ARTICLE

American Journal of PHYSICAL ANTHROPOLOGY | WILEY

Biocultural evidence of precise manual activities in an Early Holocene individual of the high-altitude Peruvian Andes

Fotios Alexandros Karakostis[1] | Hugo Reyes-Centeno[2,3,4] | Michael Franken[5] | Gerhard Hotz[6,7] | Kurt Rademaker[8] | Katerina Harvati[1,2]

[1]Paleoanthropology, Senckenberg Centre for Human Evolution and Palaeoenvironment, Department of Geosciences, University of Tübingen, Tübingen, Germany

[2]DFG (Deutsche Forschungsgemeinschaft) Center for Advanced Studies "Words, Bones, Genes, Tools," Eberhard Karls University of Tübingen, Tübingen, Germany

[3]Department of Anthropology, University of Kentucky, Lexington, Kentucky

[4]William S. Webb Museum of Anthropology, University of Kentucky, Lexington, Kentucky

[5]State Office for Cultural Heritage Baden-Württemberg, Osteology, Konstanz, Germany

[6]Anthropological Collection, Natural History Museum of Basel, Basel, Switzerland

[7]Integrative Prehistory and Archaeological Science, University of Basel, Basel, Switzerland

[8]Department of Anthropology, College of Social Sciences, Michigan State University, East Lansing, Michigan

Correspondence
Fotios Alexandros Karakostis, Paleoanthropology, Senckenberg Centre for Human Evolution and Palaeoenvironment, University of Tübingen, Tübingen 72070, Germany.
Email: afkarakostis@hotmail.com

Funding information
Alexander von Humboldt-Stiftung; Deutsche Forschungsgemeinschaft, Grant/Award Numbers: DFG CO226/20-1, DFG FOR 2237; Max Planck Institute for the Science of Human History; Northern Illinois University; Pontificia Universidad Católica del Perú

Abstract

Objectives: Cuncaicha, a rockshelter site in the southern Peruvian Andes, has yielded archaeological evidence for human occupation at high elevation (4,480 masl) during the Terminal Pleistocene (12,500–11,200 cal BP), Early Holocene (9,500–9,000 cal BP), and later periods. One of the excavated human burials (Feature 15-06), corresponding to a middle-aged female dated to ~8,500 cal BP, exhibits skeletal osteoarthritic lesions previously proposed to reflect habitual loading and specialized crafting labor. Three small tools found in association with this burial are hypothesized to be associated with precise manual dexterity.

Materials and methods: Here, we tested this functional hypothesis through the application of a novel multivariate methodology for the three-dimensional analysis of muscle attachment surfaces (entheses). This original approach has been recently validated on both lifelong-documented anthropological samples as well as experimental studies in nonhuman laboratory samples. Additionally, we analyzed the three-dimensional entheseal shape and resulting moment arms for muscle *opponens pollicis*.

Results: Results show that Cuncaicha individual 15-06 shows a distinctive entheseal pattern associated with habitual precision grasping via thumb-index finger coordination, which is shared exclusively with documented long-term precision workers from recent historical collections. The separate geometric morphometric analysis revealed that the individual's *opponens pollicis* enthesis presents a highly projecting morphology, which was found to strongly correlate with long joint moment arms (a fundamental component of force-producing capacity), closely resembling the form of Paleolithic hunter-gatherers from diverse geo-chronological contexts of Eurasia and North Africa.

Discussion: Overall, our findings provide the first biocultural evidence to confirm that the lifestyle of some of the earliest Andean inhabitants relied on habitual and forceful precision grasping tasks.

KEYWORDS

Andes, Early Holocene, entheses, muscle attachments, *opponens pollicis*

1 | INTRODUCTION

The biocultural evolution of *Homo sapiens* is characterized by environmental adaptability during dispersal across the world, which allowed early human populations to flourish across a diverse range of ecological conditions (Roberts & Stewart, 2018). One of the major objectives of bioarchaeology is to elucidate the subsistence strategies of prehistoric humans, identifying the habitual practices that led to their survival in diverse environments. In this framework, high-altitude archaeological sites show that prehistoric hunter-gatherer groups inhabited ecosystems characterized by extremely cold temperatures and hypoxia, in which human survival depends on the development of refined subsistence strategies (e.g., Aldenderfer, 2006; Ossendorf et al., 2019; Rademaker et al., 2014; Rick, 1980). Accurate reconstructions of habitual behavior in such early human communities is only feasible through the establishment of reliable associations between their biological (skeletal) and cultural remains.

One of the highest-altitude Pleistocene archaeological sites worldwide is the Cuncaicha rockshelter, located within the Pucuncho Basin of the Peruvian Andes, lying at 4,480 m above sea level. The dated occupational sequence of the site involves four different phases of human habitation, the oldest of which is dated to 12,500–11,200 cal BP. These findings demonstrate the presence of Terminal Pleistocene populations in a highly demanding environment, within ~2,000 years of the earliest lowland sites in South America. Subsequent occupations at Cuncaicha occurred during the Early Holocene (9,500–9,000 cal BP), the Late Middle Holocene, (5,700–5,000 cal BP) and the Late Holocene (<4,000 cal BP) (Rademaker et al., 2014).

Five adult human burials have been identified at Cuncaicha, including three individuals dated to the Early Holocene (9,100–8,400 cal BP), and two dated to the Late Holocene (4,290–4,080 cal BP and 3,370–3,180 cal BP) (Francken, Beier, Reyes-Centeno, Harvati, & Rademaker, 2018; Posth et al., 2018; Rademaker & Hodgins, 2018). Several isolated and undated skeletal fragments indicate the presence of additional individuals, including a subadult (Francken et al., 2018). Formal comparative craniometric analysis of the earliest Cuncaicha skull with others from throughout South America indicates morphological similarity in respiratory and masticatory components among the earliest crania studied, from Lagoa Santa, Brazil and Lauricocha Cave in the north-central Peruvian Andes (Menéndez, Rademaker, & Harvati, 2019). These findings may indicate deep-shared ancestry among these widely distributed individuals, as well as convergent morphological adaptations to high-altitude environments in the latter cases (Cuncaicha and Lauricocha). Ancient DNA analysis of the earliest individual from Cuncaicha revealed an Early Holocene lineage distinct from the Clovis-associated genome identified in other early individuals from Brazil and Chile, while two Late Holocene Cuncaicha genomes indicated a population change by about 4,200 years ago (Posth et al., 2018). This genetic change corresponds with demographic expansions into South America, possibly associated with a shift from foraging subsistence to the adoption of pastoralism in the Andes (Goldberg, Mychajliw, & Hadly, 2016; Moore, 2016; Posth et al., 2018).

Throughout its occupation sequence, the Cuncaicha rockshelter contains abundant faunal remains, demonstrating the hunting of large and small herbivores and onsite butchering and extensive processing of animal carcasses (Moore, 2013, 2016). Stone tools reflect hunting, cutting, hide working, and other tasks (Rademaker et al., 2014). Consistent with these insights from material assemblages, carbon and nitrogen stable isotope measurements of bone collagen from the five adult human skeletons buried in Cuncaicha indicate a diet with protein resources procured from the high-altitude plateau (Haller von Hallerstein, 2017).

One of the recovered skeletons, Feature 15-06, was dated to 8,537–8,386 cal BP (Rademaker & Hodgins, 2018) and belongs to a middle-aged female. This individual was found in association with two small obsidian scrapers and a bone tool bearing red ochre (Figure 1) (Francken et al., 2018). According to past experimental research on lithic implements, the production and use of similar tools for various cutting or scraping tasks requires the use of forceful precision grasping relying on the thumb and index finger (Key & Lycett, 2018; see also discussion in Karakostis, Hotz, Tourloukis, & Harvati, 2018). Such a scenario would agree with previous assessments of the habitual technology-producing activities of females from 32 ethnographic foraging societies that rely heavily on hunting for subsistence (Kelly, 2007; Murdock, 1981; Murdock & Provost, 1973; Waguespack, 2005). In these societies, women performed tasks such as house building, production of pottery, basketry, rope, and woven articles, butchery, and hide-scraping (i.e., cutting, scraping, peeling, stretching, and softening hides), many of which involve a high degree of intense manual precision (Waguespack, 2005; see also relevant case study by Becker, 2016). In all ethnographic cases where 50% or more of the diet was composed of meat, women did 100% of the hide working (Waguespack, 2005). Such a system would be expected among hunter-gatherers of the Peruvian *puna* (i.e., high-elevation grassland and shrubland ecological zone of the Andean plateau), where large and small herbivores are abundant, economically useful

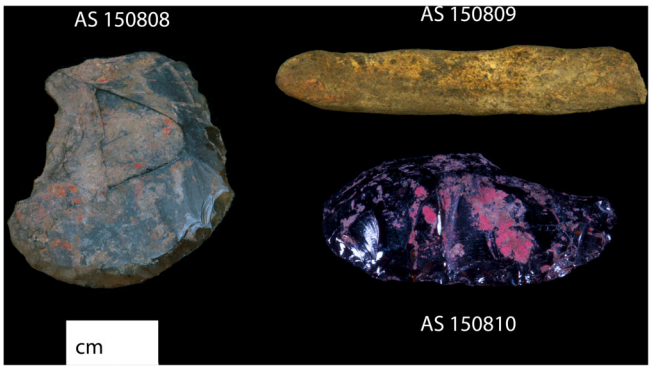

FIGURE 1 The three tools with traces of red ochre found in association with Cuncaicha individual 15-06, including two lithic scrapers (AS 150808 and AS 150810) and a potential bone crayon (AS 150809). Composite image: Erica Cooper

plants are rare, and hunting-based subsistence is well documented by the terrestrial model (Johnson, 2014) and empirical archaeological evidence (Rademaker & Moore, 2018). Importantly, a previous paleopathological analysis of Feature 15-06 conducted by some of us (Francken et al., 2018) identified a distribution of bone attrition in the skeleton that can be associated with the habitual practice of crafting labor, such as weaving or curing of hides, which require coordinated corporal movement and manual precision (Francken et al., 2018). However, the previous study emphasized that further research was required to test this biomechanical hypothesis.

The present study therefore aims to evaluate the hypothesis that the lifestyle of this early high-altitude Andean individual 15-06, relied on habitual forceful precision grasping tasks. We rely on a novel and repeatable three-dimensional (3D) approach for analyzing hand muscle attachment sites (entheses) through multivariate statistical procedures (Karakostis, Hotz, Scherf, Wahl, & Harvati, 2017; Karakostis, Hotz, Tourloukis, & Harvati, 2018; Karakostis & Lorenzo, 2016). In contrast to other approaches for analyzing entheses, this original method for reconstructing physical activity has been validated on the basis of anthropological samples with life-long occupational documentation (Karakostis et al., 2017; Karakostis, Hotz, Tourloukis, & Harvati, 2018) and with blind experimental studies different laboratory animal species (Karakostis, Jeffery, & Harvati, 2019; Karakostis, Wallace, Konow, & Harvati, 2019). In addition, considering the distinctive findings for the metacarpal enthesis of the *opponens pollicis* muscle, we use a repeatable 3D geometric morphometric approach (Karakostis, Hotz, Tourloukis, & Harvati, 2018) for quantifying its projecting shape and assessing its statistical correlation with the muscle's resulting moment arms for abduction and flexion (i.e., fundamental components of torque and biomechanical efficiency; Ward, Winters, & Blemker, 2010; Maki & Trinkaus, 2011).

2 | MATERIALS AND METHODS

2.1 | Background information

The skeletal remains of the individual 15-06 were recovered from the surface of the Terminal Pleistocene stratum in Unit 13, at approximately 80 cm depth. The 15-06 skeleton is incomplete, consisting of lower and upper limb segments, pelvic remains, four lumbar vertebrae (second–fifth) as well as several rib fragments (Francken et al., 2018). While most skeletal elements are fragmentary, hand bones are well preserved. Additional cranial elements belonging to this individual appear to have been translocated to a higher stratigraphic position ~4,000 cal BP when a seated burial was interred in Unit 13 atop individual 15-06. These cranial elements, including a mandible and molar that does not fit within the mandible, were assigned to individual 15-06 based on direct radiocarbon dates (Francken et al., 2018; Rademaker & Hodgins, 2018).

Two accelerator mass spectrometry (AMS) dates on ultrafiltered (UF) bone collagen were obtained from a distal tibia (AA107844, 7,676 ± 44 BP), and the mandible ramus (AA107846, 7,701 ± 44 BP). A third UF AMS measurement (AA109417, 7,689 ± 31 BP) was made on dentine of the molar. Based on these three concordant AMS dates, a pooled mean age of 7,689 ± 22 BP, or 8,536–8,386 cal BP (using SHCal13, Hogg et al., 2013), is assigned to individual 15-06 (Rademaker & Hodgins, 2018).

Burial 15-06 was situated on her right side with crossed legs and the upper arms alongside the body axis, which was roughly in an east to west direction. The lower left arm was angled at the elbow with the hand positioned on the pelvis, while the lower right arm was parallel to the body axis (Francken et al., 2018). Just south of individual 15-06 and at the same depth was the lower half of another burial, individual 15-05. This burial was deposited on the back with legs in a flexed and upright position. Two AMS dates on UF bone collagen provide a pooled mean age of 8,986–8,691 cal BP for individual 15-05. Bayesian modeling of the date ranges of the two adjacent early Holocene burials indicates that the lifetimes of these people did not overlap (Rademaker & Hodgins, 2018).

Individual 15-06 is a middle aged (30–50 years old) female of relatively small stature (estimated at 154 cm) (Francken et al., 2018). These demographic characteristics (sex, age, and stature) were assessed based on the individual's well-preserved pelvic and femoral traits (Francken et al., 2018). As mentioned above, individual 15-06 presented arthritic lesions across multiple joints of her skeleton, including those of the inferior lumbar spine, right hand, right wrist, left knee, and multiple foot joints (Francken et al., 2018). As far as the hand and wrist bones are concerned, individual 15-06 presented evidence of osteoarthritis (i.e., combination of osteophytes, eburnation, and microporosis) in several wrist bones (lunate, capitate, trapezium, and hamate), metacarpals, and phalanges. The frequency and intensity of osteoarthritis in the left hand is less severe than in the right (Francken et al., 2018).

Next to the right elbow joint two obsidian scrapers (AS 150808 and AS 150810) and a pointed bone tool (AS 150809) were discovered in situ (Figure 1). All three artifacts display traces of red ochre. Although small, anthropogenically introduced red ochre nodules are present in sediments spanning the Cuncaicha occupation sequence, there are only five chipped stone tools and one bone tool containing traces of red ochre within the site. That ochre-covered tools are rare in Cuncaicha, and half of the site's ochre-covered tools are found in direct association with the 15-06 burial, suggest that these objects were part of this woman's personal equipment or were purposefully placed with her burial.

Both AS 150808 and 150810 are approximately 3 cm long and 2–3 cm wide, with a thicker working surface at the distal ends of the tools and smaller proximal ends. AS 150808 is an end scraper made on a thin obsidian flake, with a steep, convex working edge typical of this tool form. AS 150810 is a multiple scraper made on a thick flake, with steep working edges on the lateral and distal margins. The manufacture of both tools involved careful, precise flaking and resharpening of working edges involving fine pressure retouch. Likely used as hide-working implements, the tools may have been hafted or hand-held. AS 150809 is an elongated bone tool fragment with polish and traces of red ochre on the pointed, rounded distal surface. The

bone tool was likely hand-held and may have been used to apply red ochre to some other material.

2.2 | Bone elements and comparative samples

Due to absence or low preservation of important muscle attachment sites on the left hand of the individual, this study focuses on the relatively complete right hand skeleton. For the purposes of this study, we selected a total of seven entheses, corresponding to eight muscles attaching onto the thumb and index finger bones (see Table 1; see detailed depictions in Karakostis & Lorenzo, 2016; Karakostis et al., 2017; Karakostis, Hotz, Scherf, Wahl, & Harvati, 2018; Karakostis, Hotz, Tourloukis, & Harvati, 2018; Karakostis, Vlachodimitropoulos, Piagkou, et al., 2018). These muscle attachment sites correspond to muscle groups that play a central role for human manual grasping movements dichotomized into power versus precision grips (Clarkson, 2000; Kivell, 2015). Previous studies have used them to successfully distinguish individuals of different lifelong occupation, differentiating, for example, laborers like stonemasons who exert primarily power-grip tasks versus workers like tailors or painters, who practice primarily precision-grasping activities (Karakostis et al., 2017; Karakostis, Hotz, Tourloukis, & Harvati, 2018). Importantly, in individual 15-06, these entheses were well-preserved and showed no pathological lesions (i.e., no osteophytic or osteolytic enthesopathies). Unfortunately, other potentially informative entheses, such as those of the fifth ray (see Karakostis et al., 2017; Karakostis, Hotz, Tourloukis, & Harvati, 2018), were damaged and, therefore, not studied further. Following Karakostis, Jeffery, and Harvati (2019), Karakostis and Lorenzo (2016), Karakostis, Wallace, et al. (2019), we developed 3D models of the muscle attachment areas using a Breuckmann SmartScan structured-light scanner (Hexagon Inc., Baden, Germany), whose structured-light technology can provide a measuring accuracy of 9 μm.

Our comparative approach relies on the use of 3D scans from 45 male skeletons belonging to the mid-19th century anthropological collection Basel-Spitalfriedhof, which is housed in the Museum of Natural History of Basel, Switzerland. These scans were developed using the same surface scanning technology (Karakostis et al., 2017). Permission for access has been officially granted by the latter institution, which is fully responsible for the curation and scientific study of these human skeletons (according to Swiss law). The lifelong occupation of these individuals is documented in detail. Furthermore, they were below 50 years old at the time of death and were not directly related. Unlike other documented anthropological collections, the archived records for our sample preserve information on the long-term occupational activities of each individual, including different professions, their durations, exact position at work (hierarchy), and hiring organizations or institutions (Hotz & Steinke, 2012; Karakostis et al., 2017). Moreover, there is archived information available on the individuals' official medical records, genealogical information, and socioeconomic data (Hotz & Steinke, 2012). Previous research applied our novel methods of entheseal analysis on this rarely documented sample and found that the multivariate patterns of hand entheses directly reflect the individuals' long-term occupational activities (Karakostis et al., 2017).

In order to provide additional insight on modern human occupational variability, we included in the comparative sample 3D models from the hand skeletons of five Paleolithic modern human individuals (two females and three males) from diverse geo-chronological contexts in Eurasia and North Africa (Table 2). These were selected because they present relatively complete and well-preserved hand bonesets, with nonpathological muscle attachment sites. Previous research conducted by some of us found that they can present distinctive power- or precision-grasping entheseal patterns (Karakostis, Hotz, Scherf, et al., 2018; see also results of this study).

2.3 | Precise delineation of entheseal 3D surfaces

The method used to define the exact borders of muscle attachment surfaces on the bones has been previously introduced and tested in Karakostis, Jeffery, and Harvati (2019), Karakostis and Lorenzo (2016), Karakostis, Wallace, et al. (2019); also see paragraph below), presenting significant intraobserver and interobserver repeatability (maximum mean error was 0.60%). Furthermore, this method is proven to show significant precision across different scanning technologies (i.e., computed-tomography scanning, laser scanning, and structured-

TABLE 1 The anatomical location of the seven entheses used and the function of their eight associated muscles

Muscles	Abbreviation	Main action	Analyzed attachment site
Abductor pollicis	ABP	Abducts the thumb	Radial base of the first proximal phalanx (same entheseal area for both muscles)
Flexor pollicis brevis	FPB	Flexes the first metacarpophalangeal joint	
Adductor pollicis	ADP	Adducts the thumb	Ulnar base of the first proximal phalanx
First dorsal *interosseous*	DI1	Abducts the second finger	Radial base of the second proximal phalanx
First palmar *interosseous*	PI1	Draws second finger towards the third finger	Ulnar base of the second proximal phalanx
Opponens pollicis	OP	Abducts, rotates, and flexes the thumb	Radial diaphysis of the first metacarpal
Flexor pollicis longus	FPL	Flexes the first distal phalanx	Palmar diaphysis of the first distal phalanx
Extensor pollicis brevis	EPB	Extends the thumb	Dorsal base of the first proximal phalanx

TABLE 2 Basic characteristics of the comparative samples used in this study, including specimen names, sex, location, and chronology in cal BP

Specimen (s)	Sex	Location	Date
Individual 15-06	Female	Peruvian Andes	8,536–8,386
Abri Pataud 3	Female	Europe	28,000–26,000
Qafzeh 9	Female	Near East	130,000–100,000 / 92,000 ka
Arene Candide 2	Male	Europe	11,800–10,900
Ohalo 2	Male	Near East	circa 19,000
Nazlet Khater 2	Male	North Africa	44,000–32,000
Basel-Spitalfriedhof Collection (45 individuals)	Males	Europe	Mid-19th century

light scanning) (Karakostis, Hotz, Scherf, et al., 2018; Karakostis, Hotz, Tourloukis, & Harvati, 2018; Karakostis, Vlachodimitropoulos, Piagkou, et al., 2018). In addition to diverse modern human samples, it has also been successfully applied on fossil hominins and laboratory animal species (rats and turkeys) (Karakostis et al., 2017; Karakostis, Hotz, Tourloukis, & Harvati, 2018; Karakostis, Jeffery, & Harvati, 2019; Karakostis & Lorenzo, 2016; Karakostis, Wallace, et al., 2019). The entire delineation process (see paragraph below) can be carried out using the tools and filtering algorithms of the open-access software Meshlab version 1.3.3 (CNR-INC, Rome, Italy).

During this procedure, the entheseal areas are digitally delineated on the bone 3D models based on surface elevation, coloration, and irregularity (Karakostis et al., 2017; Karakostis, Hotz, Tourloukis, & Harvati, 2018; Karakostis, Jeffery, & Harvati, 2019; Karakostis & Lorenzo, 2016; Karakostis, Wallace, et al., 2019). The exact steps of the applied protocol are illustrated in Figure 2. Among these three criteria, the most important one is the presence of distinctive surface elevation (i.e., projecting or depressed bone surface). Evaluating these criteria is carried out with the assistance of 3D imaging filters that color-map the surface of the bone depending on its coloration (i.e., using Meshlab's "equalize vertex colors" filter; Figure 2b) and/or its elevation and irregularity (i.e., using surface curvature filters available in Meshlab, such as "discrete curvatures"; Figure 2c). Subsequently, for optimal use of these filters in defining the exact borders of entheses on the bone, the observer should apply them on a bone region that encompasses the muscle attachment site as well as its immediately surrounding bone area (i.e., a flatter zone of surface circulating the enthesis; see Figure 2d), using filters such as "curvature principal directions" or "calculation of geodesic distances" within entheseal areas (Figure 2e). Finally, the flatter area surrounding the entheseal surface (i.e., dark blue zone in Figure 2e) is virtually removed and the resulting 3D area is computed in square mm (Figure 2f) or extracted as PLY files for geometric morphometric analysis (see last section of Section 2).

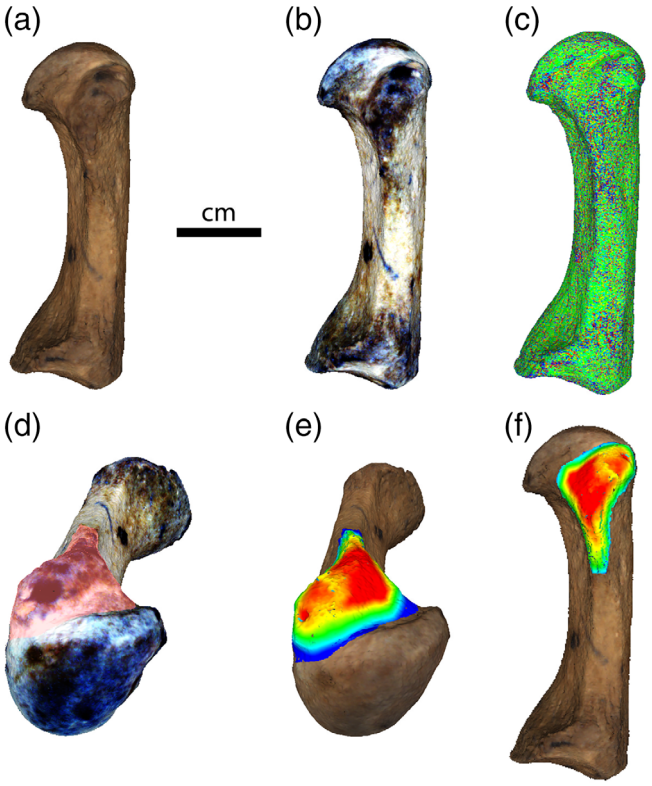

FIGURE 2 A step-by-step summary of the protocol applied for delineating the 3D areas of entheses on the bones, previously introduced and tested by Karakostis, Jeffery, and Harvati (2019), Karakostis and Lorenzo (2016), Karakostis, Wallace, et al. (2019). The example depicted corresponds to the insertion site of muscle *opponens pollicis* in the right first metacarpal of Feature 15-06, from a lateral (a, b, c, and f; distal is up) or proximolateral (d and e; distal is down) point of view. The process includes the development of high-resolution 3D surface models (a), color filtering using the filter "equalize vertex colors" (b), surface curvature filtering using the filter "discrete curvatures" (c), selection of the entheseal surface in addition to a thin zone of flatter surrounding "normal" bone area (d), determination of the exact borders of entheses using the filter "curvature principal directions" or "calculation of geodesic distances" (e), cropping of the surrounding flatter bone area (i.e., blue zone in panel e), and calculation of entheseal surface size in square mm (f). The resulting 3D area can also be exported for precise landmark-based 3D shape analysis (Karakostis, Hotz, Tourloukis, & Harvati, 2018)

2.4 | Multivariate 3D analysis of muscle synergy groups

Following our recently developed approach (Karakostis et al., 2017), the resulting surface area measurements (in square mm) were adjusted for overall size using the geometric mean approach (Mosimann, 1970; Jungers,

Falsetti, & Wall, 1995; e.g., see Almecija, Moya-Sola, & Alba, 2010; Karakostis et al., 2017; Karakostis, Hotz, Tourloukis, & Harvati, 2018; Karakostis, Jeffery, & Harvati, 2019 for applications to hand bones). This specimen-by-specimen technique has been recommended as a highly efficient way for isometrical size adjustment (Elewa, 2010; Lycett, Cramon-Taubadel, & Foley, 2006). Following this approach, each entheseal measurement (in square mm) was divided by the geometric mean of all seven measurements from the same individual (Almecija et al., 2010; Karakostis et al., 2017). Therefore, the resulting values represent each entheseal area's proportion of the individual's geometric mean (Figure 3).

The adjusted measurements of all seven entheses were used as variables in a principal component analysis (PCA), without any prior group assumptions for the individuals (Figure 4). A correlation matrix was used due to distinctive ranges among variables. The seven variables met all basic assumptions for a PCA, including sample size requirements (a minimum of five specimens per variable), approximately normal distribution (based on normal probability plots; Field, 2013), and no significant outliers (based on the z-scores approach; Field, 2013). The number of principal components (PCs) plotted was decided based on the scree-plot approach (Cattell, 1966; Field, 2013).

2.5 | Analysis of *opponens pollicis*' entheseal 3D shape and muscle moment arms

The entheseal patterns exhibited by 15-06 were characterized by the great proportional size of the attachment for *opponens pollicis* (Figure 3; Tables 1 and 3), a muscle of central importance for thumb opposition and precision grasping. Therefore, we investigated whether the 3D shape of this individual's enthesis was proportionally more projecting, possibly providing the attaching muscle with greater moment arm lengths and force-producing capacities (Karakostis, Hotz, Scherf, et al., 2018; Karakostis, Hotz, Tourloukis, & Harvati, 2018; Karakostis, Vlachodimitropoulos, Piagkou, et al., 2018; Maki & Trinkaus, 2011; Ward et al., 2010); also see arguments in Section 4). For this objective, we employed a recent approach for analyzing entheses using landmark-based 3D geometric morphometrics (Karakostis, Hotz, Tourloukis, & Harvati, 2018) with verified intraobserver and interobserver precision (i.e., landmark placement error was less than 4% across landmarks; Karakostis, Hotz, Tourloukis, & Harvati, 2018).

Briefly, the delineated and cropped 3D surfaces of entheses (PLY files) were imported into the Geomorph package of R-CRAN (Adams & Otárola-Castillo, 2013). Then, following the approach of Karakostis, Hotz, Scherf, et al., 2018; Karakostis, Hotz, Tourloukis, & Harvati, 2018; Karakostis, Vlachodimitropoulos, Piagkou, et al., 2018, we digitized a total of six geometrically defined landmarks at the outline of the enthesis (Figure 5). Based on these fixed points, we calculated a set of 30 equidistant semilandmarks on the entheseal surfaces, which were allowed to slide along tangent planes on the 3D surface following a minimum bending energy criterion (Adams, Rohlf, & Slice, 2013). Subsequently, we applied Procrustes superimposition on the raw coordinates of the 36 landmarks, in order to transform them into Procrustes coordinates and use them as variables for a shape

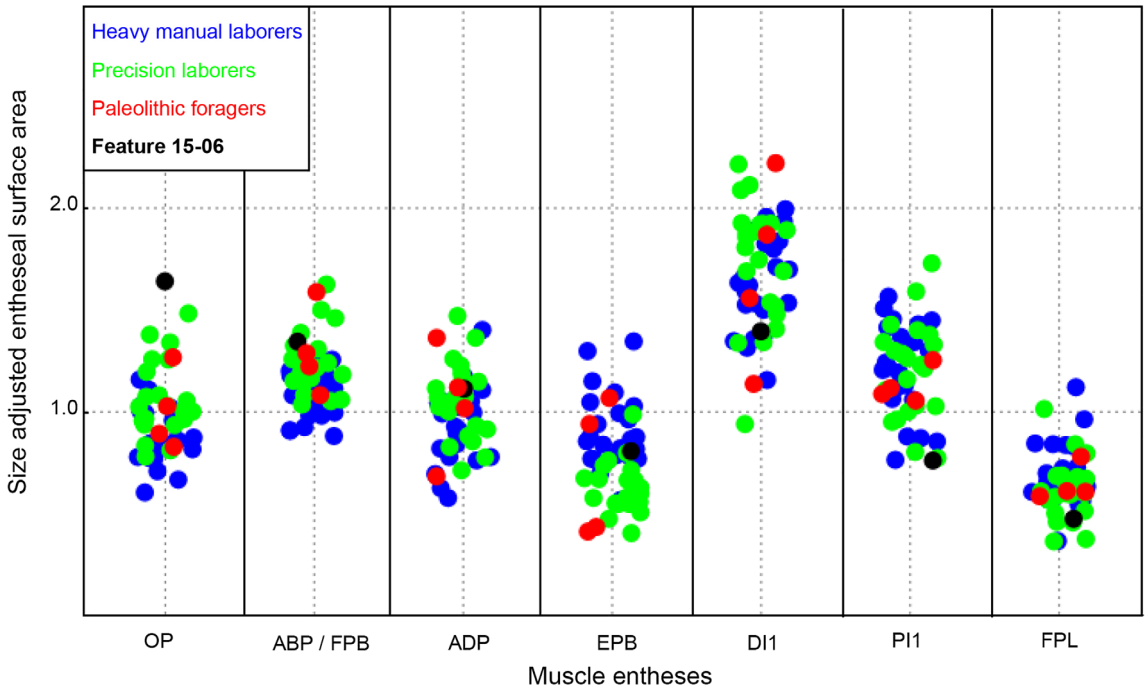

FIGURE 3 Jitter plots showing the entheseal surface values (square mm) for Cuncaicha 15-06 (black) and the comparative samples across seven muscles, after adjusted for size using the geometric mean. The entheses of the four thenar muscles—and especially that of *opponens pollicis*—are proportionally high. The muscles abbreviated are *opponens pollicis* (OP), *abductor pollicis/flexor pollicis brevis* (ABP/FPB), *adductor pollicis* (ADP), *extensor pollicis brevis* (EPB), *dorsal interosseous* 1 (DI1), *palmar interosseous* 1 (PI1), and *flexor pollicis longus* (FPL)

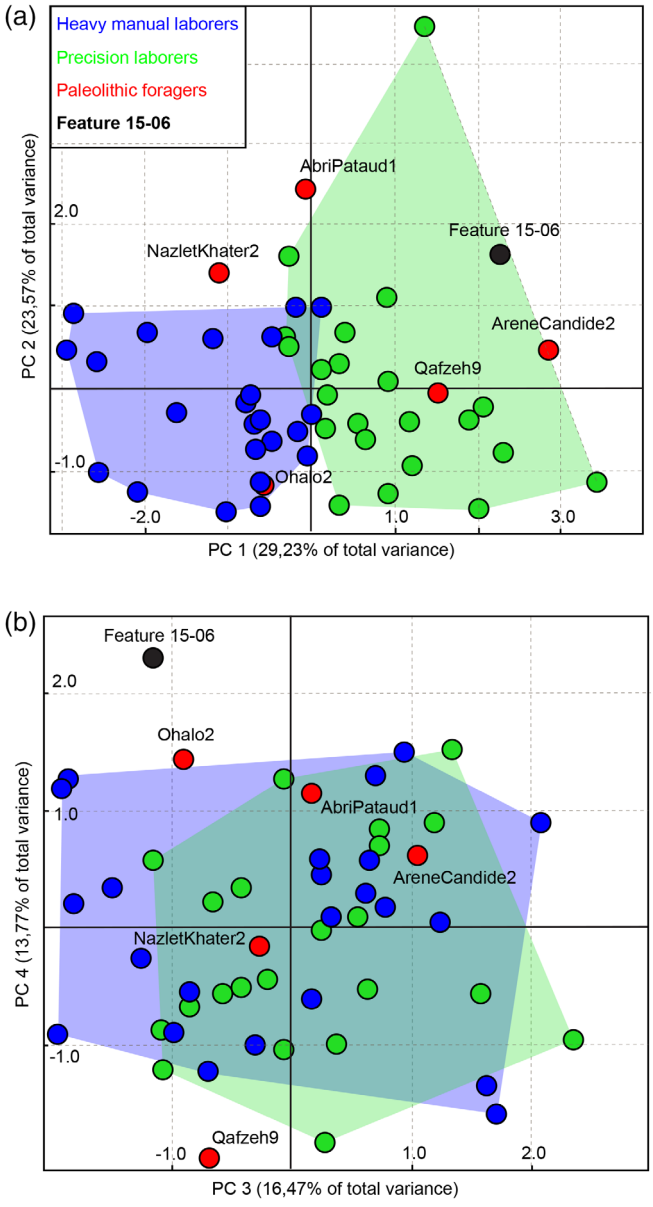

FIGURE 4 Plots of the correlation principal component analysis based on seven entheseal variables (size-adjusted surface measurements) and all 51 individuals: (a) principal component 1 to principal component 2, with sample legend and (b) principal component 3 to principal component 4. No prior group assumptions were made but convex hulls were added a posteriori for visualization

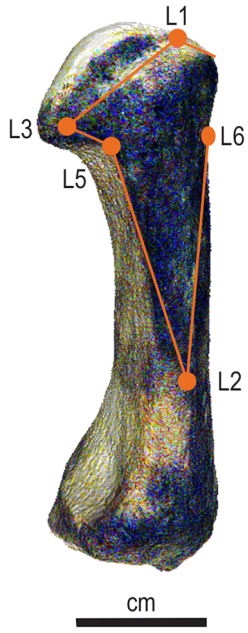

FIGURE 5 Lateral view of a male right thumb metacarpal from the mid-19th century Basel-Spitalfriedhof collection (distal is up), indicating the locations of the six geometrically defined landmark points on the insertion enthesis of *opponens pollicis*, which were used in the geometric morphometric analysis. These comprised the basis for calculating 30 surface sliding semilandmarks

PCA (Figure 6). Shape changes were visualized using warped surfaces (using the thin-plate spline method), following Adams et al. (2013).

In addition, to verify that greater entheseal projection for *opponens pollicis* influences joint torque by regulating moment arm lengths (Maki & Trinkaus, 2011; Ward et al., 2010), we estimated these for each individual hand skeleton in our samples using the 3D models of their metacarpals and associated trapezia. Moment arms were calculated for both actions of *opponens pollicis* (Maki & Trinkaus, 2011; Marzke et al., 1999), involving thumb abduction (see side illustration in Figure 7) and flexion (see bottom illustration in Figure 8) at the carpometacarpal joint. Both processes were carried out using the software Avizo (Thermo Fisher Scientific Inc., Waltham, MA). First, we virtually placed the two bones in full articulation and increased the distance between their adjoining articular surfaces by 1.5 mm (i.e., the mean inter-articular joint space for the

TABLE 3 Statistics of the correlation principal component analysis based on seven entheseal variables (size-adjusted surface measurements) and all 51 individuals. For muscle abbreviations, see Table 1

			Factor loadings						
Principal component	Eigenvalue	Variance explained (%)	OP	ABP/FPB	ADP	EPB	FPL	DI1	PI1
1	2.05	29.23	0.61	0.78	0.36	−0.74	−0.55	0.30	−0.04
2	1.65	23.57	0.35	0.02	0.54	−0.14	0.60	−0.74	−0.56
3	1.15	16.47	0.19	−0.03	−0.32	−0.48	0.36	−0.33	0.74
4	0.96	13.77	0.56	0.19	−0.65	0.35	−0.07	−0.16	−0.22
Total		83.03							

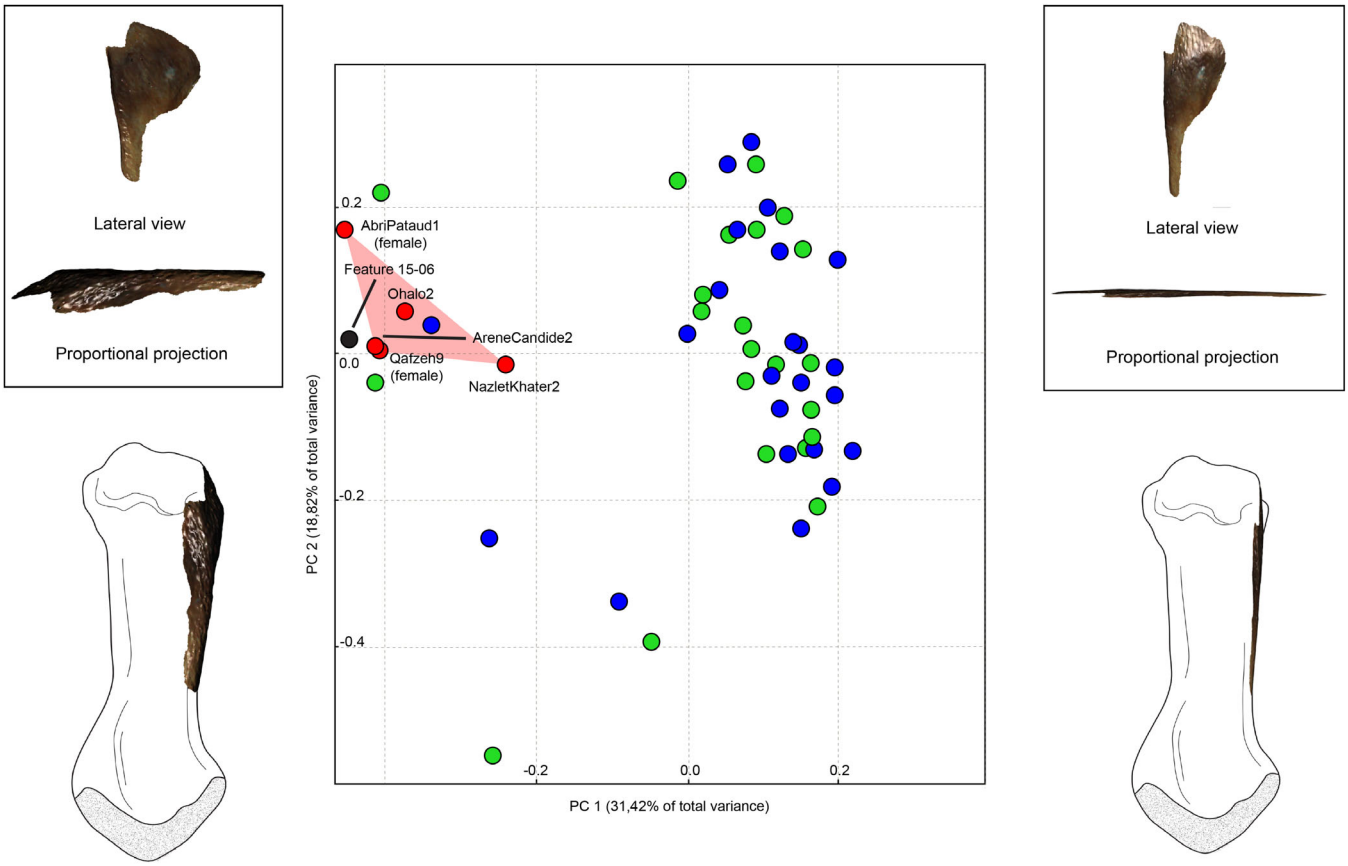

FIGURE 6 Plot of the shape principal component analysis of the 3D insertion area of muscle *opponens pollicis* (principal components 1 and 2). Individuals were colored by group following the sample legend of Figures 3 and 4 (i.e., Cuncaicha 15-06: black, Eurasian Paleolithic foragers: red, lifelong precision laborers: green, lifelong heavy manual laborers: blue). The upper side figures represent the pattern of shape variation along the first principal component based on the visualization technique of warped surfaces (Adams et al., 2013), while the lower side illustrations of metacarpals (palmar aspect, distal is up) demonstrate how these shape differences represent the degree of entheseal projection away from the surrounding bone area (the muscle's line of force is depicted in Figures 7 and 8). Factor loadings are provided in Table 3

thumb's carpometacarpal joint in modern humans; Koff, Ugwonali, Strauch, Rosenwasser, & Ateshian, 2003). Subsequently, as demonstrated in Figures 7 and 8, we drew a vector representing the muscle's line of action, which was defined by linking the most central point of the muscle's origin enthesis on the trapezium's tubercle with the most central point of the metacarpal's insertion site. The most central point of each enthesis was defined as its geometric center, virtually calculated using the tools of the Avizo software. For the metacarpal insertion site, this was typically located within the most elevated region of the attachment surface area (e.g., see bottom illustration of Figure 8). In cases where the trapezium was not preserved or unavailable (i.e., for fossil individual Arene Candide 2), the likely position of the trapezium tubercle was approximated. The resulting lines of action in our samples (e.g., see illustrations in Figures 7 and 8) reflect those indicated and/or depicted in previous biomechanical and morphological research on this muscle (Maki & Trinkaus, 2011; Marzke et al., 1999). Then, after virtually defining the geometric center of the intrajoint space area (i.e., the axis of rotation), we quantified moment arm by measuring its perpendicular distance to the muscle's line of force action (Lieber & Ward, 2011; Ward et al., 2010), both for abduction (see side illustration of Figure 7) as well as flexion (see side illustration of Figure 8) at the carpometacarpal joint. Given that moment arm is affected by the overall size of individuals, we also calculated "relative moment arm" by dividing each moment arm value by the corresponding metacarpal bone length (see Katzenberg & Grauer, 2018), which was also measured in mm using Avizo. For each muscle action (abduction or flexion), we assessed the degree of correlation between entheseal shape (PC1 scores) and moment arm (both raw and relative values) using the Spearman's Rho coefficient (Field, 2013). Moreover, for each of the two muscle actions, we compared raw and relative moment arm between the 45 recent modern humans and the 6 early foragers using Mann–Whitney *U* tests. These nonparametric tests were preferred due to normality violations. For ensuring measuring repeatability, all moment arms

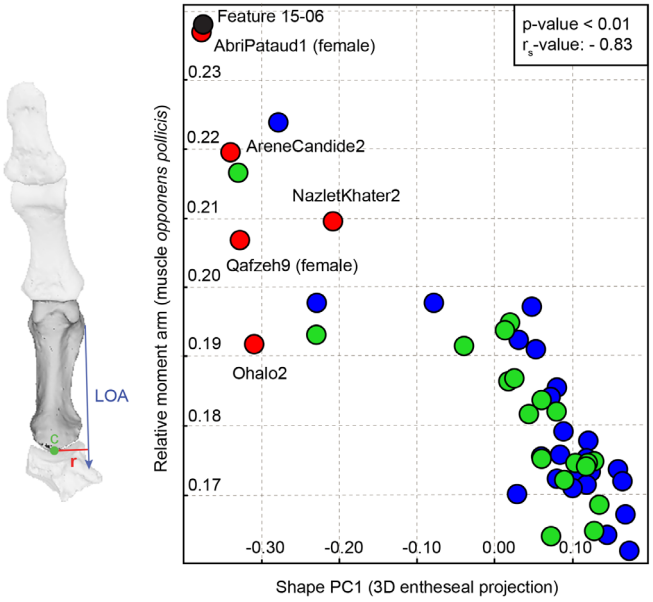

FIGURE 7 Left: A summary of the technique applied for measuring each individual's abduction moment arm (r) for muscle *opponens pollicis*, after virtually defining the muscle's line of action (LOA) and axis of rotation (C). The exact steps of the process are described in Section 2. The thumb bone 3D models are shown from a palmar point of view and correspond to individual 15-06's right trapezium, metacarpal, proximal phalanx, and distal phalanx (from bottom to up). Right: Bivariate plot of shape principal component 1 (shape PC1) versus relative moment arm, including the significant output of the Spearman's Rho correlation test (upper right side of the plot). The results of the test before size-adjustment are outlined in Section 3. Relative moment arm was calculated by diving the raw measurements by the corresponding metacarpal length (see Section 2)

were measured twice by the same author (F. A. K.) and the intraobserver error was found to range between 0 and 3.66%.

3 | RESULTS

As demonstrated in Figure 3, the size-adjusted entheseal measurements of the thenar muscles (i.e., the insertion sites of *opponens pollicis*, *adductor pollicis brevis*, and the common insertion area of *abductor pollicis brevis* and *flexor pollicis brevis*) are relatively large in Cuncaicha individual 15-06. The most striking value is that of the insertion site of *opponens pollicis*, a muscle of fundamental contribution to thumb opposition for numerous power and precision grasping tasks (Karakostis et al., 2017; Karakostis, Hotz, Tourloukis, & Harvati, 2018; Kivell, 2015). For that enthesis, 15-06 has the highest size-adjusted value across our prehistoric and recent samples. By contrast, the other four entheses are proportionally small in comparison to other individuals. Nevertheless, these low values are mainly the effect of size-adjusting using the geometric mean for each individual (see in Karakostis, Jeffery, & Harvati, 2019. Essentially, the scores of these four entheses appear proportionally low for individual 15-06 due to the unusually high values of the three thenar entheses.

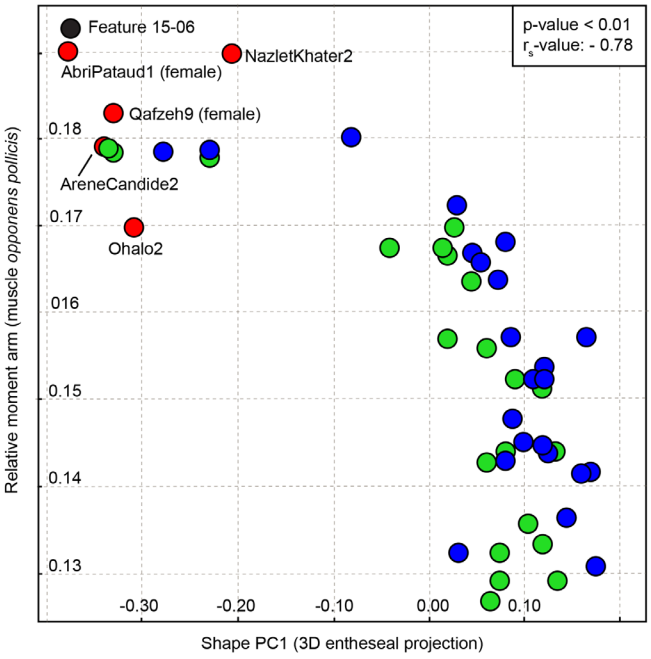

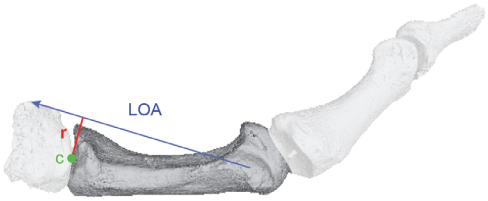

FIGURE 8 Below: A summary of the technique applied for measuring each individual's flexion moment arm (r) for muscle *opponens pollicis*, after virtually defining the muscle's line of action (LOA) and axis of rotation (C). The exact steps of the process are described in Section 2. The thumb bone 3D models are shown from a lateral point of view (palmar is up) and correspond to individual 15-06's right trapezium, metacarpal, proximal phalanx, and distal phalanx (from left to right). Above: Bivariate plot of shape principal component 1 (shape PC1) versus relative moment arm, including the significant output of the Spearman's Rho correlation test (upper right side of the plot). The results of the test before size-adjustment are outlined in Section 3. Relative moment arm was calculated by diving the raw measurements by the corresponding metacarpal length (see Section 2)

3.1 | Multivariate 3D analysis focusing on muscle synergy groups

We ran a PCA on the size-adjusted variables to identify potential multivariate correlations across entheses that may link 15-06 with a distinctive muscle synergy group and/or occupational tendency (Karakostis et al., 2017). Based on the recommendation of the scree-plot technique (Field, 2013), we plotted four PCs, representing 83.03% of total variance in the sample (Figure 4). Our multivariate approach revealed a main axis of variance (i.e., PC1; 29.23% of total variance) where scores clearly differentiated long-term heavy manual workers (presenting a power-grasping entheseal pattern) from lifelong

workers of lower intensity and more precise daily labor (showing a precision-grasping entheseal pattern involving the thumb and index finger) (Figure 4a). Early modern humans show both positive and negative PC1 values. Specifically, two of them show a precision grasping pattern, another two exhibit a power-grasping pattern, and one presents an intermediate PC1 score (Figure 4a).

Individual 15-06 shows a very high positive PC1 value that reflects a strong multivariate correlation among her entheses for the thumb's thenar muscles and the first dorsal interosseous muscle of the index finger (see Figure 4a and Table 3). This distinctive score causes 15-06 to overlap exclusively with lifelong precision workers, such as professional tailors and painters (Karakostis et al., 2017), and to clearly differ from lifelong heavy manual laborers (i.e., construction workers). The scores on PC2 and PC3 are less informative for the purposes of this study, as they represent entheseal patterns that show extensive overlapping across all groups (Figure 4 and Table 3). Finally, the value of Feature 15-06 on PC4 (13.77% of total variance) is indicative of a proportionally very large enthesis for muscle *opponens pollicis*, which differentiates this individual from all recent and prehistoric specimens of the sample (Figure 4b).

3.2 | *Opponens pollicis*' entheseal 3D shape and biomechanical efficiency

Considering that both our univariate and multivariate approaches highlighted the distinctively large proportional size of the *opponens pollicis*' enthesis (Figures 3 and 4a; Table 3), we carried out a separate 3D analysis to investigate its shape characteristics (Figure 6) and whether they correlate with the attaching muscle's moment arm for abduction (Figure 7) and flexion (Figure 8). In contrast to the results of the multivariate analyses focusing on the relationship among different entheses (Figure 4), the 3D shape analysis of the metacarpal enthesis of *opponens pollicis* showed extensive overlapping between the two occupational groups, in all shape PCs (Figure 6). Variation along PC1 (31.42% of sample variance) represents shape differences in the degree of entheseal surface projection and breadth (see depicted shape changes in the side illustrations of Figure 6). The remaining shape PCs were not depicted because they presented extensive overlapping across all populations and occupational groups, without providing relevant information on the shape attributes of 15-06.

Along with a few recent modern humans, all prehistoric foragers in our sample showed high negative PC1 values, reflecting relatively elevated and wide entheseal surfaces. The scores of shape PC1 were found to be strongly correlated with the attaching muscle's moment arm, both for abduction (Figure 7) as well as flexion (Figure 8). When focusing on abduction (Figure 7), the correlation was strong both when using raw moment arm measurements (p-value <.01; r_s-value: −.78) as well as size-adjusted values (p-value <.01; r_s-value: −.83) (Figure 7). Individuals 15-06 and Abri Pataud 1 (Upper Paleolithic female from Europe) share similarly long moment arms (9.78 and 9.49 mm, respectively) and extreme negative PC1 scores. The significant differences in abduction moment arm between recent modern humans (mean: 7.61 mm; *SD*: 0.77) and early foragers (mean: 8.94 mm; *SD*: 0.71) was confirmed by the results of the Mann–Whitney *U* tests, both on the raw measurements (p-value <.01; *U*-value: 18) and the size-adjusted values (p-value <.01; *U*-value: 41.5). The average difference between the groups was 17.41 and 22.22%, respectively. Similarly, regarding thumb flexion, a strong and negative correlation was found between shape PC1 and raw (p-value <.01; r_s-value: −.73) as well as size-adjusted (p-value <.01; r_s-value: −.78) moment arm estimations. Again, female individuals 15-06 and Abri Pataud 1 presented very long moment arms (7.91 and 7.63 mm, respectively). The Mann–Whitney *U* tests indicated a statistically significant difference in flexion moment arms between early foragers (mean: 7.57 mm; *SD*: 0.22) and recent modern humans (mean: 6.44 mm; *SD*: 0.76), both when using raw moment arm measurements (p-value <.01; *U*-value: 20) as well as size-adjusted values (p-value <.01; *U*-value: 9). The mean difference between the groups was 17.55 and 20.00%, respectively.

4 | DISCUSSION

4.1 | Evidence for habitual precision grasping behavior

Previous research hypothesized that the Peruvian high-altitude individual 15-06 from Cuncaicha shows a distribution of bone attrition in her skeleton that could be the result of intense crafting physical activities relying on coordinated corporal movement and manual precision. This hypothesis, which aligns with the interpretation of habitual activities in Paleoindian hunter-gatherer communities derived from modern ethnographic paradigms (Waguespack, 2005), is also supported by the discovery of three small associated tools (Figure 1), whose manufacture and use would require a certain degree of precision grasping involving the thumb and the index finger (e.g., Key & Lycett, 2018). Based on the literature, such habitual tasks could have involved lithic tool knapping, food processing (e.g., cutting, defleshing, and disarticulating animal carcasses), or hide processing for garment making (Marzke, 2013; Key & Lycett, 2018; also see Karakostis, Hotz, Tourloukis, & Harvati, 2018). Similar associations between bone attrition and precise crafting labor have also been made for more recent female individuals from other high-altitude archaeological sites (e.g., Becker, 2016). For instance, a recent study of a middle-aged female from the Bolivian highlands (Tiwanaku culture, ~1,000 cal BP) reported a very similar distribution of osteoarthritis in the skeleton (Becker, 2016). The hand remains from that burial presented osteoarthritis particularly at the thumb and index finger joints, while the enthesis of *opponens pollicis* on the pollical metacarpal was pronounced. Based on the artifacts associated with this burial, as well as the surrounding archaeological context, Becker (2016) linked the above osteological characteristics with the habitual performance of precise crafting labor (likely pottery making or weaving).

Similarly, the Cuncaicha individual 15-06 is also a middle-aged female presenting an osteoarthritis distribution that possibly reflects

precise crafting labor body postures (Francken et al., 2018). The findings of our two separate analyses indicate that this individual shows a proportionally large and projecting attachment site for muscle *opponens pollicis* (Figures 3 and 6), together with a multivariate pattern among entheseal surface areas that directly reflects a precision-grasping muscle synergy group involving the thumb and the index finger (Figure 4a). Such a precision-grasping pattern was only found among habitual precision workers of a recent historical sample with lifelong occupational documentation (e.g., professional long-term tailors or painters). In this study, the separation between the dichotomized occupational tendencies of power versus precision grasping groups appears to be slightly lower than in our previous research on the same reference sample (Karakostis et al., 2017), as observed in the PCA analysis involving different entheseal surface areas (Figure 4a). This slight discrepancy is due to the exclusion of two entheses of the fifth ray as a result of their bad preservation in individual 15-06 (see Section 2).

4.2 | Biomechanical implications of the 3D shape analysis (*opponens pollicis*)

Based on our previous anthropological and animal laboratory studies on entheses (Karakostis et al., 2017; Karakostis, Jeffery, & Harvati, 2019; Karakostis, Wallace, et al., 2019), physical activity can be accurately predicted using multivariate analyses that focus on correlations among different entheses of muscles that act synergistically. In contrast, directly comparing the morphology of each entheseal structure across distinct individuals or groups seems to be more prone to the effects of numerous factors of entheseal variability, such as gene variants, biological age, body size, hormones, nutrition, and others (Karakostis, Jeffery, & Harvati, 2019; Schrader, 2019). This observation is consistent with the present study's findings on the 3D shape of the metacarpal enthesis of *opponens pollicis* (Figure 6), which showed clear overlap between heavy manual laborers and precision workers (in contrast to our multivariate analyses; see Figure 4).

Even though that 3D geometric morphometric analysis of a single enthesis was not informative on the individuals' habitual grasping tendencies, it revealed that Feature 15-06's *opponens pollicis* attachment is highly projecting away from the surrounding metacarpal bone surface and its joints (see side illustrations of Figure 6 depicting entheseal variation relative to surrounding bone area; also see Figures 7 and 8). That trait was shared with Paleolithic hunter-gatherers from diverse geographic and chronological contexts (Eurasia and North Africa), as well as a few robust recent individuals from Basel (Figure 6; Table 2). More importantly, our analyses showed that this relative bone projection is strongly correlated with the attaching muscle's moment arms (for abduction and flexion), which significantly differ between early foragers and our recent human sample (see Results). This association occurs because greater bone surface elevation at this muscle attachment site directly increases moment arm lengths and naturally affects joint torque (see side illustration of Figure 7 and bottom illustration of Figure 8), which is mathematically defined as the product of muscle force and moment arm (Lieber & Ward, 2011). Joint torque comprises a direct indicator of biomechanical efficiency and force-producing capacity (Ward et al., 2010). On this basis, our results suggest that a diverse group of Paleolithic foragers and the Early Holocene Andean individual 15-06 shared an increased force-producing capacity for thumb opposition, which has been suggested as a vital component of Paleolithic subsistence practices for either power- or precision-grasping movements (Key & Lycett, 2018; Maki & Trinkaus, 2011; Niewoehner, 2006). Furthermore, the observed strong correlations between moment arms and entheseal 3D morphology (Figures 7 and 8) provide original evidence for the functional importance of the *opponens pollicis*' muscle attachment area and its direct contribution to biomechanical efficiency (Maki & Trinkaus, 2011).

Previous work on human cadaveric hands has questioned the connection between entheses and biomechanical efficiency by reporting no statistical linear association between muscle attachment size and the maximum force-producing capacities of the attaching muscle (represented by the physiological cross-sectional area; Williams-Hatala, Hatala, Hiles, & Rabey, 2016). However, the individuals used in that work were of advanced biological age (mean of 77.9 ± 12 years old), a factor known to deteriorate the mechanisms of activity-induced muscle remodeling, as well as entheseal bone change (Foster, Buckley, & Tayles, 2014; Maïmoun & Sultan, 2011). Fundamentally, such analyses and interpretations do not consider entheseal bone projection and the associated muscles' moment arm lengths, which comprises one of the two fundamental components of biomechanical efficiency (Ward et al., 2010). Such a strategy is limited because it has been biomechanically demonstrated that torque can vary substantially due to moment arm differences, even when comparing two identical muscles that exert the same exact forces (e.g., Lieber & Ward, 2011; Ward et al., 2010). Essentially, the results of the present study (Figures 7 and 8) demonstrate that, even if a muscle's maximum force-generating capacity was indeed not associated with the raw 3D size of the associated enthesis (Williams-Hatala et al., 2016), the attachment's position on the bone and degree of relative projection can still directly influence moment arms and, thus, net force production (Figures 7 and 8).

Furthermore, given that larger muscle units (i.e., greater physiological cross-sectional areas) produce higher muscle forces that tend to be less controllable during manipulation (Clarkson, 2000), one would expect that precise manual activities mostly rely on relatively smaller muscle forces that can be more accurately directed and coordinated. For such muscle contractions, a longer moment arm would serve to amplify the net power of such lower -but more easily controlled muscle forces. On this basis, considering the results for Feature 15-06 in the two distinct analyses of this study, it is possible that the habitual precise grasping behavior of this individual (indicated by the 3D multivariate analysis; Figure 4) was combined with an ability to produce thumb opposition movements that could be forceful but perhaps more precisely coordinated (indicated by the 3D shape analysis and strong moment arm correlations; Figures 7 and 8). Nonetheless, it must be emphasized that longer moment arms for *opponens pollicis* would comprise a biomechanical advantage both for precision as well

as power-grasping movements relying on thumb opposition (e.g., those reflected on the entheses of other forager individuals in Figure 4).

4.3 | The effects of sexual dimorphism and future research horizons

We note that our thoroughly documented comparative sample is currently restricted to one sex within a single population. In light of the functional mechanisms described above, we expect that including females in our comparative sample would yield a similar entheseal separation between individuals exerting primarily power grips versus those exerting primarily precision grasping in their occupations. Aspects of sexual dimorphism in entheses are described primarily in terms of entheseal size (Foster et al., 2014; Karakostis & Lorenzo, 2016; Karakostis, Zorba, & Moraitis, 2014), where males tend to have larger muscle attachments than females. Because our approach focuses either on entheseal multivariate patterns (i.e., proportions among size-adjusted surface area measurements) or 3D shape coordinates (geometric morphometric analysis), and in light of the archaeological context of the 15-06 burial, we consider our interpretations to be robust. Furthermore, it is worth noting that both the male and the female prehistoric foragers of our sample shared similar 3D shape attributes (Figures 6–8), while the occurrence of power- and precision-grasping entheseal patterns in both sexes has been previously verified in past applications of our multivariate entheseal approach (Karakostis & Lorenzo, 2016).

Nevertheless, future work specifically addressing variation, including sexual dimorphism in other geographically and temporally diverse populations of known lifelong occupation, will serve to refine our results. In addition, the inclusion of individuals from other Early to Middle Holocene archaeological sites in the central Andean region, such as Quiqché, Quipa Pucusana, or Santo Domingo (Beynon & Siegel, 1981), where similar patterns of degenerative osteological changes have been reported, will further enhance our understanding of manual activities and foraging strategies in the region.

5 | CONCLUSIONS

The results of our study provide original biocultural evidence of precise manual activities in one of the oldest archaeological contexts of the Peruvian highlands. By proposing a meaningful link between individual 15-06's habitual grasping performance, arthritic lesions, and associated artifacts, our findings confirm predictions about the precise manual tasks of early New World female hunter-gatherers (Waguespack, 2005). Furthermore, the highly projecting entheseal 3D shapes and relatively long moment arms for muscle *opponens pollicis* in 15-06 and other prehistoric hunter-gatherers are directly indicative of high force-generating capacity for thumb opposition. Overall, we argue that such subsistence and crafting practices were vital for the survival of early human hunter-gatherer groups, such as those inhabiting the Peruvian Andes. Given that similar activity patterns are also observed in much later archaeological contexts from this area (e.g., see Becker, 2016), as well as among recent hunter-gatherer groups (Waguespack, 2005), our observations provide support for the value of ethnographic evidence in making biomechanical inferences for past populations based on skeletal activity markers.

ACKNOWLEDGMENTS

The authors are deeply grateful to the following institutions and researchers for granting them access to fossil specimens and/or 3D data: Tel Aviv University (H. May and I. Hershkovitz), National Museum of Natural History in Paris (Grimaud-Hervé, F. Detroit, and M. Friess), and the Italian Ministry of Cultural Heritage and Activities (as well as the Museo Archeologico Del Finale and V. Sparacello for collecting data from the remains of Arene Candide). Moreover, the hand skeleton of Nazlet Khater 2 was digitized thanks to the Agence Nationale de la Recherce (ANR) project "Big Dry" (ANR-14-CE31). The authors are grateful to the coordinator F. Bon and the partners I. Crevecoeur, D. Pleurdeau, J. Lesur, and C. Tribolo for providing them with access to the virtual material of Nazlet Khater 2. The 2015 field season in Cuncaicha was funded by the Max Planck Institute for the Science of Human History, the Pontifical Catholic University of Peru, Northern Illinois University, the Alexander von Humboldt Foundation, and the German Research Foundation (DFG FOR 2237: Project "Words, Bones, Genes, Tools: Tracking Linguistic, Cultural, and Biological Trajectories of the Human Past"). The authors thank many participants of the 2015 field season at Cuncaicha rockshelter and the Peruvian Ministry of Culture for fieldwork, collections analysis, and sample export permits (Resoluciónes Directorales #353-2015 and #900016-2018, and Resolución Viceministerial 092-2016). Marko Lopez at the Peruvian Ministry of Culture office in Arequipa, Cecilia Mauricio, and Peter Kaulicke provided invaluable assistance in exporting the Cuncaicha material for analysis in Germany. The authors thank Judith Beier, Abel Bosman, María López Sosa, Carolin Röding, and Panagiotis Zodos for assistance with curation of the Cuncaicha skeletal material. The authors also thank the Department of Early Prehistory and Quaternary Ecology, Eberhard Karls Universität Tübingen, for access to scanning instrumentation that was made available through a grant from the German Research Foundation (DFG CO226/20-1). Special thanks should be given to the volunteers of the "Citizen Science Project Basel Spitalfriedhof" (Universität Basel), for their important work on the detailed documentation of this study's reference sample. Open access funding enabled and organized by Projekt DEAL.

CONFLICT OF INTEREST

The authors declare no conflict of interest.

AUTHOR CONTRIBUTIONS

Fotios Alexandros Karakostis: Conceptualization; formal analysis; investigation; methodology; project administration; software; supervision; validation; visualization; writing-original draft; writing-review

and editing. **Hugo Reyes-Centeno**: Data curation; investigation; resources; writing-review and editing. **Michael Francken**: Investigation; writing-review and editing. **Gerhard Hotz**: Data curation; investigation; project administration; resources; supervision; writing-review and editing. **Kurt Rademaker**: Conceptualization; data curation; formal analysis; funding acquisition; investigation; methodology; project administration; resources; supervision; visualization; writing-review and editing. **Katerina Harvati**: Conceptualization; funding acquisition; investigation; project administration; resources; supervision; writing-review and editing.

DATA AVAILABILITY STATEMENT

The data that support the findings of this study (i.e., the hand bone 3D models of individual 15-06) are openly available in Dryad at https://doi.org/10.5061/dryad.dbrv15f04. The 3D models from the other early foragers of our sample cannot be shared based on our existing permits. Nevertheless, their obtained size and shape measurements are available from the corresponding author upon reasonable request.

ORCID

Fotios Alexandros Karakostis https://orcid.org/0000-0003-3913-4332

Katerina Harvati https://orcid.org/0000-0001-5998-4794

REFERENCES

Adams, D., Rohlf, F., & Slice, D. (2013). A field comes of age: Geometric morphometrics in the 21st century. *Hystrix, the Italian Journal of Mammalogy*, *21*, 7–14.

Adams, D. C., & Otárola-Castillo, E. (2013). geomorph: An r package for the collection and analysis of geometric morphometric shape data. *Methods in Ecology and Evolution*, *4*(4), 393–399.

Aldenderfer, M. (2006). Modelling plateau peoples: The early human use of the World's high plateaux. *World Archaeology*, *38*(3), 357–370.

Almecija, S., Moya-Sola, S., & Alba, D. M. (2010). Early origin for human-like precision grasping: A comparative study of pollical distal phalanges in fossil hominins. *PLoS One*, *2010*, e11727.

Becker, S. (2016). Skeletal evidence of craft production from the Ch'iji Jawira site in Tiwanaku, Bolivia. *Journal of Archaeological Science: Reports*, *9*, 405–415.

Beynon, D. E., & Siegel, M. I. (1981). Ancient human remains from Central Peru. *American Antiquity*, *46*(1), 167–178.

Cattell, R. B. (1966). The scree test for the number of factors. *Multivariate Behavioral Research*, *1*, 245–276.

Clarkson, H. M. (2000). *Musculoskeletal assessment: Joint range of motion and manual muscle strength*. Dallas, TX: Lippincott Williams & Wilkins.

Elewa, A. M. T. (2010). *Morphometrics for nonmorphometricians*. New York, NY: Springer.

Field, A. (2013). *Discovering statistics using SPSS (4th revised edition)*. London, England: SAGE Publications.

Foster, A., Buckley, H., & Tayles, N. (2014). Using enthesis robusticity to infer activity in the past: A review. *Journal of Archaeological Method and Theory*, *21*(3), 511–533. https://doi.org/10.1007/s10816-012-9156-1

Francken, M., Beier, J., Reyes-Centeno, H., Harvati, K., & Rademaker, K. (2018). The human skeletal remains from the Cuncaicha rock shelter, Peru. In *New perspectives on the peopling of the Americas* (pp. 125–153).

Goldberg, A., Mychajliw, A. M., & Hadly, E. A. (2016). Post-invasion demography of prehistoric humans in South America. *Nature*, *532* (7598), 232–235.

Haller von Hallerstein, S. (2017). *Multi-isotopic paleo-diet reconstruction of hunter-gatherer in the Peruvian Puna*. (Unpublished Masterthesis). University of Tuebingen.

Hogg, A., Turney, C., Palmer, J., Southon, J., Kromer, B., Ramsey, C. B., … Jones, R. (2013). The New Zealand kauri (*Agathis australis*) research project: A radiocarbon dating intercomparison of Younger Dryas wood and implications for IntCal13. *Radiocarbon*, *55*(4), 2035–2048.

Hotz, G., & Steinke, H. (2012). Knochen, skelette, krankengeschichten: Spitalfriedhof und spitalarchiv—zwei sich ergänzende quellen. *Basler Zeitschrift Für Geschichte Und Altertumskunde*, *112*, 105–138.

Johnson, A. L. (2014). Exploring adaptive variation among hunter-gatherers with Binford's frames of reference. *Journal of Archaeological Research*, *22*(1), 1–42.

Jungers, W. L., Falsetti, A. B., & Wall, C. E. (1995). Shape, relative size, and size-adjustments in morphometrics. *American Journal of Physical Anthropology*, *38*(S21), 137–161.

Karakostis, F. A., Zorba, E., & Moraitis, K. (2014). Osteometric sex determination using proximal foot phalanges from a documented human skeletal collection. *Anthropologischer Anzeiger*, 403–427.

Karakostis, F. A., Hotz, G., Scherf, H., Wahl, J., & Harvati, K. (2017). Occupational manual activity is reflected on the patterns among hand entheses. *American Journal of Physical Anthropology*, *164*(1), 30–40.

Karakostis, F. A., Hotz, G., Scherf, H., Wahl, J., & Harvati, K. (2018). A repeatable geometric morphometric approach to the analysis of hand entheseal three-dimensional form. *American Journal of Physical Anthropology*, *166*(1), 246–260.

Karakostis, F. A., Hotz, G., Tourloukis, V., & Harvati, K. (2018). Evidence for precision grasping in Neandertal daily activities. *Science Advances*, *4*(9), eaat2369. https://doi.org/10.1126/sciadv.aat2369

Karakostis, F. A., Jeffery, N., & Harvati, K. (2019). Experimental proof that multivariate patterns among muscle attachments (entheses) can reflect repetitive muscle use. *Scientific Reports*, *9*(1), 1–9. https://doi.org/10.1038/s41598-019-53021-8

Karakostis, F. A., & Lorenzo, C. (2016). Morphometric patterns among the 3D surface areas of human hand entheses. *American Journal of Physical Anthropology*, *160*(4), 694–707. https://doi.org/10.1002/ajpa.22999

Karakostis, F. A., Vlachodimitropoulos, D., Piagkou, M., Scherf, H., Harvati, K., & Moraitis, K. (2018). Is bone elevation in hand muscle attachments associated with biomechanical stress? A histological approach to an anthropological question. *The Anatomical Record*, *302* (7), 1093–1103. https://doi.org/10.1002/ar.23984

Karakostis, F. A., Wallace, I. J., Konow, N., & Harvati, K. (2019). Experimental evidence that physical activity affects the multivariate associations among muscle attachments (entheses). *Journal of Experimental Biology*, *222*(23).

Katzenberg, M. A., & Grauer, A. L. (2018). *Biological anthropology of the human skeleton*. Oxford, England: Wiley.

Kelly, R. J. (2007). *The foraging spectrum: Diversity in hunter-gatherer lifeways (reprint)*. New York, NY: Eliot Werner Publications.

Key, A. J. M., & Lycett, S. J. (2018). Investigating interrelationships between lower Palaeolithic stone tool effectiveness and tool user biometric variation: Implications for technological and evolutionary changes. *Archaeological and Anthropological Sciences*, *10*(5), 989–1006. https://doi.org/10.1007/s12520-016-0433-x

Kivell, T. L. (2015). Evidence in hand: Recent discoveries and the early evolution of human manual manipulation. *Philosophical Transactions of the Royal Society B: Biological Sciences*, *370*(1682), 20150105. https://doi.org/10.1098/rstb.2015.0105

Koff, M. G., Ugwonali, O. F., Strauch, R. J., Rosenwasser, M. P., & Ateshian, V. C. (2003). Sequential wear patterns of the articular cartilage of the thumb carpometacarpal joint in osteoarthritis. *Journal of Hand Surgery*, *28*, 597–604.

Lieber, R. L., & Ward, S. R. (2011). Skeletal muscle design to meet functional demands. *Philosophical Transactions of the Royal Society B:*

Biological Sciences, *366*(1570), 1466–1476. https://doi.org/10.1098/rstb.2010.0316

Lycett, S. J., Cramon-Taubadel, N., & Foley, R. A. (2006). A crossbeam coordinate caliper for the morphometric analysis of lithic nuclei: A description, test, and empirical examples of application. *Journal of Archaeological Science*, *33*, 847–861.

Maïmoun, L., & Sultan, C. (2011). Effects of physical activity on bone remodeling. *Metabolism: Clinical and Experimental*, *60*(3), 373–388. https://doi.org/10.1016/j.metabol.2010.03.001

Maki, J., & Trinkaus, E. (2011). *Opponens Pollicis* mechanical effectiveness in Neandertals and early modern humans. *Paleoanthropology*, *2011*, 62–71.

Marzke, M. W. (2013). Tool making, hand morphology and fossil hominins. *Philosophical Transactions of the Royal Society B: Biological Sciences*, *368*(1630), 20120414. https://doi.org/10.1098/rstb.2012.0414

Marzke, M. W., Marzke, R. F., Linscheid, R. L., Smutz, P., Steinberg, B., Reece, S., & An, K. N. (1999). Chimpanzee thumb muscle cross sections, moment arms and potential torques, and comparisons with humans. *American Journal of Physical Anthropology*, *110*, 163–178.

Menéndez, L. P., Rademaker, K., & Harvati, K. (2019). Revisiting east–west skull patterns and the role of random factors in South America: Cranial reconstruction and morphometric analysis of the facial skeleton from Cuncaicha Rockshelter (southern Peru). *PaleoAmerica*, *5*(4), 315–334. https://doi.org/10.1080/20555563.2019.1703167

Moore, K. M. (2013). Large mammal Zooarchaeology at Cuncaicha: Exploration of research potential. Unpublished report.

Moore, K. M. (2016). Early domesticated camelids in the Andes. In J. M. Capriles (Ed.), *The archaeology of Indian pastoralism*. New Mexico:University of New Mexico Press. (pp. 17–38).

Mosimann, J. E. (1970). Size allometry: Size and shape variables with characterizations of the lognormal and generalized gamma distributions. *Journal of the American Statistical Association*, *65*(330), 930–945.

Murdock, G. P. (1981). *Atlas of world cultures*. Pittsburgh, PA: University of Pittsburgh Press.

Murdock, G. P., & Provost, C. (1973). Factors in the division of labor by sex: A cross-cultural analysis. *Ethnology*, *12*(2), 203–225. https://doi.org/10.2307/3773347

Niewoehner, W. A. (2006). Neanderthal hands in their proper perspective. In J.-J. Hublin, K. Harvati, & T. Harrison (Eds.), *Neanderthals revisited: New approaches and perspectives*. New York: Springer (pp. 157–190). https://doi.org/10.1007/978-1-4020-5121-0_9

Ossendorf, G., Groos, A. R., Bromm, T., Tekelemariam, M. G., Glaser, B., Lesur, J., … Miehe, G. (2019). Middle Stone Age foragers resided in high elevations of the glaciated Bale Mountains, Ethiopia. *Science*, *365* (6453), 583–587. https://doi.org/10.1126/science.aaw8942

Posth, C., Nakatsuka, N., Lazaridis, I., Skoglund, P., Mallick, S., Lamnidis, T. C., … Reich, D. (2018). Reconstructing the deep population history of Central and South America. *Cell*, *175*(5), 1185–1197. e22. https://doi.org/10.1016/j.cell.2018.10.027

Rademaker, K., & Hodgins, G. (2018). Exploring the chronology of occupations and burials at Cuncaicha rockshelter. In K. Harvati, G. Jäger, & H. Reyes-Centeno (Eds.), *New perspectives on the peopling of the Americas* (pp. 107–124). Töbingen: Kerns Verlag.

Rademaker, K., Hodgins, G., Moore, K., Zarrillo, S., Miller, C., Bromley, G. R. M., … Sandweiss, D. H. (2014). Paleoindian settlement of the high-altitude Peruvian Andes. *Science (New York, N.Y.)*, *346* (6208), 466–469. https://doi.org/10.1126/science.1258260

Rademaker, K., & Moore, K. M. (2018). Variation in the occupation intensity of early forager sites of the Andean puna: Implications for settlement and adaptation. In A. K. Lemke (Ed.), *Foraging in the past: Archaeological studies of hunter-gatherer diversity* (pp. 76–118). Boulder, CO: University Press of Colorado.

Rick, J. W. (1980). *Prehistoric hunters of the high Andes*. Academic Press.

Roberts, P., & Stewart, B. A. (2018). Defining the 'generalist specialist' niche for Pleistocene *Homo sapiens*. *Nature Human Behaviour*, New York. *2*(8), 542–550. https://doi.org/10.1038/s41562-018-0394-4

Schrader, S. (2019). *Activity, diet and social practice: Addressing everyday life in human skeletal remains*. New York: Springer. https://doi.org/10.1007/978-3-030-02544-1

Waguespack, N. M. (2005). The organization of male and female labor in foraging societies: Implications for Early Paleoindian archaeology. *American Anthropologist*, *107*(4), 666–676. https://doi.org/10.1525/aa.2005.107.4.666

Ward, S. R., Winters, T. M., & Blemker, S. S. (2010). The architectural design of the gluteal muscle group: Implications for movement and rehabilitation. *The Journal of Orthopaedic and Sports Physical Therapy*, *40*(2), 95–102. https://doi.org/10.2519/jospt.2010.3302

Williams-Hatala, E. M., Hatala, K. G., Hiles, S., & Rabey, K. N. (2016). Morphology of muscle attachment sites in the modern human hand does not reflect muscle architecture. *Scientific Reports*, *6*(1), 1–8. https://doi.org/10.1038/srep28353

How to cite this article: Karakostis FA, Reyes-Centeno H, Franken M, Hotz G, Rademaker K, Harvati K. Biocultural evidence of precise manual activities in an Early Holocene individual of the high-altitude Peruvian Andes. *Am J Phys Anthropol*. 2021;174:35–48. https://doi.org/10.1002/ajpa.24160